Radiation defects in ion-implanted silicon. II. Mössbauer spectroscopy of ^{119}Sn defect structures from implantations of radioactive tellurium

A. Nylandsted Larsen,* G. Weyer, and L. Nanver
Institute of Physics, University of Aarhus, DK-8000 Aarhus C, Denmark
(Received 31 January 1979)

Defect structures containing Sn impurity atoms in silicon have been studied by Mössbauer emission spectroscopy on the 24-keV transition of ^{119}Sn. The defects have been produced by ion implantation of radioactive ^{119m}Te. This decays via the decay chain $^{119m}\text{Te} \rightarrow {}^{119}\text{Sb} \rightarrow {}^{119}\text{Sn}$ to the Mössbauer level of ^{119}Sn. In the Mössbauer spectra the ^{119}Sn atoms yield six different lines, characterized primarily by their isomer shifts and Debye-Waller factors. The existence of six independent lines and some of their properties are established experimentally by varying implantation dose and temperature, from postimplantations of other selected isotopes, from implantations in silicon crystals with a range of oxygen concentrations, and from annealing experiments. The lines have been attributed to different Sn bonding configurations and assigned to several lattice locations of the impurity atoms. In all spectra the line characteristic of substitutional Sn atoms was observed (isomer shift: $\delta = 1.84$ mm/s, Debye temperature: $\Theta = 250$ K). Large fractions of the impurity atoms are found in vacancy associated defect structures. Different impurity-vacancy complexes have been distinguished from the isomer shifts (electronic configurations) and Debye temperatures of the Sn impurity atoms ($\delta = 2.6$ mm/s, $\Theta = 165$ or 250 K, and $\delta = 0.9$ mm/s, $\Theta = 230$ K). Possible configurations of these complex defects are discussed. A minor fraction of the Sn atoms ($\delta = 3.3$ mm/s, $\Theta = 250$ K) is concluded to be in an interstitial position, probably in an agglomerate. A line ($\delta = 4.4$ mm/s and $\Theta = 175$ K) correlated with the oxygen content of the sample is assigned to a complex defect structure containing oxygen atoms. From the implantation and annealing experiments, conclusions on properties of the Te and Sb parents can be drawn. The fraction of Te atoms ending on undisturbed substitutional sites is found to vary with the implantation temperature (~70 at.% for 670 K and ~30 at.% for room-temperature implantations). The remaining atoms are distributed in different defect structures. Annealing of room-temperature-implanted samples up to ~1200 K did not change the Te-atoms locations substantially. Thus, defect structures containing Te atoms are concluded to be unusually stable. In contrast to this, the related defect structures containing Sb atoms from the radioactive decay of Te can be annealed at temperatures between 500 and 900 K.

I. INTRODUCTION

It is well known that tellurium as an impurity in elemental group-IV semiconductors creates deep levels in the forbidden energy gap.[1,2] These impurity centers can have a large influence on the electrical and optical properties of the semiconductors even when found in very small concentrations; but the fundamental knowledge about deep levels in semiconductors is, however, still rudimentary (for a recent review of deep level impurities in semiconductors, see Ref. 3). The creation of deep levels, together with the observation of high substitutional fractions of Te in Si,[1,4–7] render this system a very promising one for technological applications. The use of ion implantation as a method to introduce deep level impurities in silicon circumvents the problem of a low solid solubility of these impurities in silicon, an effect which complicates heavy doping of silicon by conventional techniques such as thermal diffusion. However, inherent to ion implantation as a doping technique is the creation of radiation damage. Complicated damage structures can be produced during the implantation process of the energetic ions. The nature of these structures is still largely unknown.

Mössbauer spectroscopy has proven to be a powerful method for studies of implanted impurity atoms in substitutional and defect sites in solids. Isotopes with suitable Mössbauer γ transitions exist for many elements. These can be implanted into solids and used as probe atoms for a study of their microscopic structure as an implanted impurity atom. The Mössbauer isotopes are fairly evenly distributed through the periodic system, which often makes it possible to find a suitable candidate in the group of elements which might be of interest. In addition,

many Mössbauer levels are populated by the decay of several different parent isotopes, which extends the number of elements applicable in such experiments. For a detailed discussion of the prospects of Mössbauer spectroscopy in studies of the microscopic structure of implanted impurity atoms in solids, the reader is referred to recent reviews on this topic.[8,9] In the present investigation radioactive ^{119m}Te has been implanted into silicon. The ^{119m}Te decays to ^{119}Sb which decays to the Mössbauer level of ^{119}Sn (see decay scheme, Fig. 1). Thus from the point of view of the complexity of the decay scheme, these experiments can be regarded as an extension of those with implantations of radioactive ^{119}Sb (see preceding paper, referred to as Part I). In particular, for a new type of annealing and postimplantation experiment reported in this paper, which utilizes the radioactive decay chain ^{119m}Te → ^{119}Sb → ^{119}Sn, the results from Part I will explicitly be applied in the interpretations.

Much confusion exists about the location of implanted Te in Si. From channeling investigations, substitutional fractions covering the range from 30 to 70 at.% have been reported, while the remaining nonsubstitutional fraction could not be located at any distinct interstitial position.[1,4,5] Mössbauer experiments on implanted radioactive Te in group-IV elements with diamond structure utilizing the 28-keV Mössbauer transition of ^{129}I(Ge, Si, diamond)[6] or the 36-keV Mössbauer transition of ^{125}Te(Ge)[10] show two broad lines with approximately equal intensities. In both studies it was concluded that approximately 50% of the implanted Te atoms occupied substitutional positions, while the remaining 50% should be in tetrahedral interstitial positions. The present investigation agrees with the channeling studies, since the substitutional fraction is found to vary between ~30 and ~70 at.% depending on the implantation conditions. The remaining nonsubstitutional fraction is found to be distributed over different sites in the host lattice.

Preliminary reports on parts of this work have been given previously (Refs. 7, 11, and 12).

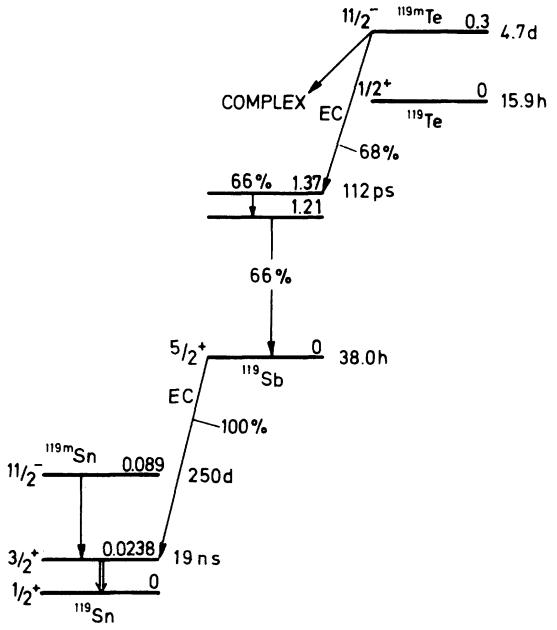

FIG. 1. Main lines of the decay scheme of ^{119m}Te.

II. EXPERIMENTAL PROCEDURE

Implantations of radioactive ^{119m}Te($T_{1/2}$=4.76 d) were carried out with an electromagnetic isotope separator at an energy of 60 keV and implantation temperatures of 300–700 K. This energy corresponds to a projected range of ~300 Å. Because of a low and not measurable ion current for mass number 119 during the ^{119m}Te implantations only an upper limit of 10^{13} atoms/cm^2 can be given for the implanted dose from the ion current during the separation. For an area of ~1 cm^2, this dose yielded source strengths between 0.5 and 2 μCi, corresponding to $\lesssim 10^{11}$ ^{119m}Te atoms/cm^2. Since it was of interest to study the effects of doses higher than 10^{11} atoms/cm^2, in some samples stable ^{125}Te was im-

TABLE I. ^{119m}Sn and ^{119m}Te implanted in silicon single crystals. [Floating zone (FZ), n type, 5–7 Ω cm.] The isomer shift δ is given relative to SnO_2, the linewidths have been fixed to 1.0 mm/s, the intensities are normalized to $\sum_i I_i = 1$.

Impl. impurity	Impl. dose (at./cm^2)	Impl. temp. (K)	line 1 δ_1 (mm/s)	I_1	line 2 δ_2 (mm/s)	I_2	line 3 δ_3 (mm/s)	I_3	line 4 δ_4 (mm/s)	I_4	line 5 δ_5 (mm/s)	I_5
^{119m}Sn	8×10^{14}	673	...		1.84(3)	1.0	...		...		...	
^{119m}Te	5×10^{14}	723	0.92[a]	0.14(3)	1.84[a]	0.49(4)	2.61[a]	0.17(3)	3.30[a]	0.08(3)	4.41[a]	0.12(3)

[a]Fixed parameter in least-squares fit. The isomer shift values are uncorrected for a possible geometrical velocity error of $\lesssim|-4\%|$.

TABLE II. ^{119m}Te implanted in silicon. Dose and implantation temperature dependence. The following Debye-Waller factors have been used to estimate the population of sites: $f_1=0.40$, $f_2=0.46$, $f_3=0.18$, $f_4=0.47$, and $f_5=0.13$. Intensities normalized to $\sum_i P_i=1$. All implantations have been performed into n-type FZ-silicon single crystals (5 Ω cm), cut perpendicular to the ⟨100⟩ axes.

Impl. dose (at./cm^2)	Impl. temp. (K)	line 1 I_1	P_1	line 2 I_2	P_2	line 3 I_3	P_3	line 4 I_4	P_4	line 5 I_5	P_5
$<10^{13}$	293	0.03(2)	0.02	0.49(5)	0.27	0.45(5)	0.63	0.04(2)	0.02	0.03(2)	0.04
5×10^{14}[a]	293	0.02(2)	0.01	0.47(5)	0.27	0.40(5)	0.60	0.06(3)	0.03	0.04(2)	0.08
$<10^{13}$	673	. . .	. . .	0.85(4)	0.68	0.12(4)	0.25	0.02(2)	0.02	0.02(2)	0.06
5×10^{14}[a]	673	0.06(3)	0.06	0.85(4)	0.68	0.06(3)	0.12	0.03(2)	0.02	0.04(2)	0.11

[a]Postimplantation of stable ^{125}Te to this dose.

planted immediately after the ^{119m}Te implantation into the same area. In Tables I and II the total doses of implanted Te atoms are stated. The dose rates of the ^{119m}Te implantations were always less than 3×10^9 atoms/cm^{2}s. A typical dose rate for the ^{125}Te implantation was 1×10^{11} atoms/cm^{2}s.

Single-crystal samples of n-type silicon were implanted. The crystals, cut perpendicular to a major axis, were tilted by ~7° relative to the beam axis to avoid implantations in channeled directions. All crystals were polished mechanically and treated chemically in mixtures of HNO_3 and HF prior to implantation.

Radioactive ^{119m}Te was obtained from a bombardment of natural tin with 20-MeV α particles from the cyclotron at the Niels Bohr Institute in Copenhagen. The bombarded material was treated chemically in order to separate the tellurium as described in Part I.

The Mössbauer spectrometer, detectors, and calibration procedure have been described in previous publications[13,14] (see also Part I).

The postannealing of the implanted samples was performed in a quartz-tube furnace with flowing dry N_2. After the annealing, the samples were cooled down to room temperature in approximately 5 min in a dry N_2 flow. In all the isochronal annealing experiments the annealing time was 20 min.

III. EXPERIMENTAL RESULTS AND DATA TREATMENT

A. Spectra

A typical Mössbauer spectrum measured at room temperature from ^{119m}Te implanted in Si (dose 5×10^{14} atoms/cm^2, implantation temperature 723 K) is shown in Fig. 2. For comparison, a room-temperature spectrum of ^{119m}Sn implanted in Si is also shown (dose 8×10^{14} atoms/cm^2, implantation temperature 723 K). It is well known that for such implantation conditions, a relatively low level of radiation damage is achieved in the implanted volume.[13] All the spectra have been analyzed by a least-squares-fit procedure assuming lines of Lorentzian shapes. In this procedure known parameters of the absorber material (SnO_2), quadrupole splitting, and linewidth have been taken into account. In most of the computer fits, one or more of the parameters have been fixed in value (i.e., the isomer shift δ, the linewidth Γ, or the line intensity I); this is indicated in Table I by an asterisk.

The fit to the experimental data for the ^{119m}Sn implant [Fig. 2(b)] is a two-line fit because of the quad-

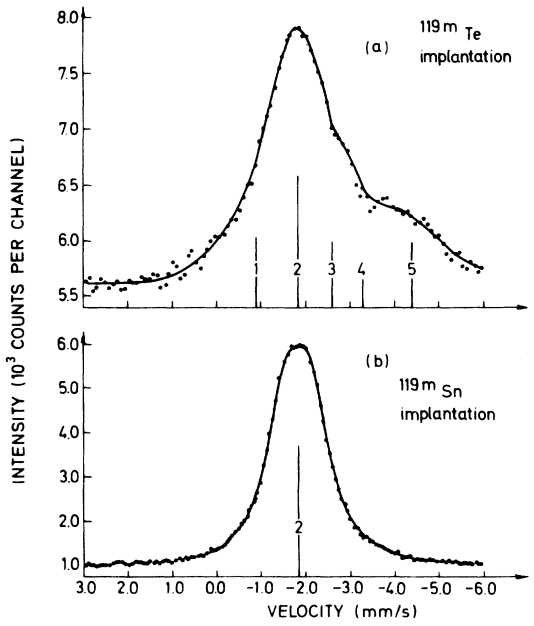

FIG. 2. Mössbauer spectra measured at room temperature of ^{119m}Te (a) and ^{119m}Sn (b) implanted in silicon at 723 K with similar doses ($5-8\times10^{14}$ atoms/cm^2). The curves represent fit to the data in terms of emission lines as indicated by the bars.

rupole splitting of the SnO_2 absorber material. The splitting of the two lines and their intensity ratio have been fixed to values obtained from measurements with standard sources ($BaSnO_3$, Mg_2Sn). Thus, only the isomer shift, the linewidth, and the line intensity have been varied in this fit. The data indicate that a single, slightly broadened line is emitted from the source. This line is known to originate from tin impurity atoms on undisturbed substitutional lattice sites.[13,14]

The Mössbauer spectrum from the ^{119m}Te implant [Fig. 2(a)] is seen to be broadened and asymmetric as compared to the spectrum of the ^{119m}Sn implant and the right-hand part of the spectrum is clearly structurized. This spectrum has been fitted assuming five emission lines, labeled line 1, line 2, . . . , line 5 (in the order of decreasing Doppler velocity and hence increasing isomer shift). One of these lines (line 2) is the well-known substitutional line from the ^{119m}Sn implants,[13] and two of the other lines (lines 3 and 4) belong to defect sites which also have been observed for ^{119}Sb implants (see Part I). A discussion of the reliability of the assumption of five emission lines for this spectrum assigned to different sites for the impurity atoms is postponed to Sec. IV. The positions and relative intensities of the five lines are indicated in the figure for this particular implant and are summarized in Table I. In the fit, the values of the isomer shifts and the widths of the lines have been fixed to average values extracted from all the experimental data reported here (see beginning of Sec. IV). As all measured spectra could be fitted satisfactorily with the same set of parameters (isomer shifts and linewidths), this fitting procedure seems to be justified even if the resolution and/or the statistical accuracy in a single spectrum may not be sufficient to establish the presence of all five lines.

B. Dose and implantation-temperature dependence

The results from implantations of ^{119m}Te in silicon single crystals for different doses and temperatures are summarized in Table II. The implanted silicon single-crystal slices were all cut from the same piece of material. Table II gives the measured intensities for the five lines I_i and the relative number of corresponding defects, P_i (with $\sum_i P_i = 1.0$). the P_i's are extracted from the intensities and the experimentally determined Debye-Waller factors (see Sec. III C) by making use of the proportionality between the measured intensity of a line I_i and the product of the relative defect numbers belonging to the line P_i and the Debye-Waller factor of the site f_i.

Because the population of sites 1, 4, and 5 is relatively low in these four implantations, the data are not conclusive as to their dependence on implantation conditions. However, the data seem to indicate that no strong dependence exists either on the implanted dose or on the implantation temperature for these lines, despite the fact that doses of $\gtrsim 10^{14}$ atoms/cm^2 implanted at room temperature render the implanted volume amorphous. A dependence on the implantation temperature is found for the two lines labeled 2 and 3. In a room-temperature implantation, around 60% of the atoms are in the site 3 and only around 30% in the site 2 (substitutional site). The opposite is the case for an implantation at 673 K ($\sim$70% in site 2, 10–20% in site 3). For these two sites, no strong dependence on the implanted dose is found in the investigated dose range ($\lesssim 10^{13}$ to 5×10^{14} atoms/cm^2), except for a weak dose dependence of the line 3 in the high-temperature implantations. It should be noted that the solid solubility of Te in silicon is exceeded for a dose of about 10^{12} atoms/cm^2.[15]

C. Low-temperature measurements

For a ^{119m}Te room-temperature-implanted silicon single crystal (dose $\lesssim 10^{13}$ atoms/cm^2), low-temperature measurements have been performed in the temperature range from 4 to 300 K. Typical Mössbauer spectra for different temperatures are shown in Fig. 3. The measured intensities for the lines are summarized in Table III. Only a very low intensity was found for line 1 in this particular implantation. Thus no conclusion as to a temperature dependence of this line could be drawn; the line has therefore been omitted in the table.

The accuracy of the intensities given in Table III does not allow a detailed interpretation in terms of the impurity lattice dynamics. Instead an interpretation based on the Debye model has been attempted. By using this model, only gross features of the lattice dynamics of the impurity atoms are expected to be reproduced.[16]

In the harmonic approximation, the Debye-Waller factor is given by

$$f = \exp(-1/3\,\mu^2\langle u^2\rangle) \ ,$$

where μ is the wave vector of the γ ray, and $\langle u^2\rangle$ is the mean-square vibrational amplitude of the emitting or absorbing nucleus. A simple one parametrization of the temperature dependence of the Debye-Waller factor can be obtained from the Debye model. This leads to[17]

$$f = \exp\left\{-\frac{6E_R}{k\Theta}x\left[\frac{1}{4}+\left(\frac{T}{\Theta}\right)^2\int_0^{\Theta/T}\frac{x\,dx}{e^x-1}\right]\right\} \ , \quad (1)$$

where E_R is the recoil energy of the daughter nucleus, Θ is the characteristic Debye temperature, and T is the absolute temperature. For a substitutional impurity in a simple mass defect model, the charac-

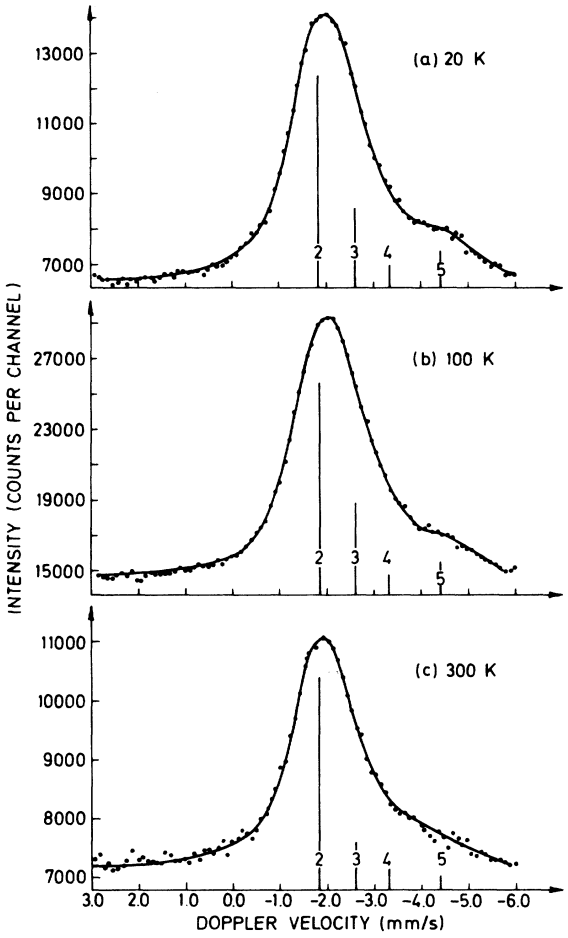

FIG. 3. (a)–(c) Mössbauer spectra of ^{119m}Te in silicon measured at different temperatures. The curves represent fits to the data in terms of four emission lines as indicated by the bars.

teristic Debye temperature Θ^I, extracted from the temperature dependence of the Debye-Waller factor is related to that of the host Θ^H, by $\Theta^I = (M_H/M_I)^{1/2}\,\Theta^H$, where M_H and M_I are the masses of the host and impurity atoms, respectively.[18] At high and low temperatures, respectively, Eq. (1) can be approximated by

$$f = \begin{cases} \exp(-6E_R T/k\Theta^2) & T \geq \frac{1}{2}\Theta \ , \quad (2) \\ \exp(-3E_R/2k\Theta) & T \approx 0 \ . \quad (3) \end{cases}$$

From the measured intensities of a line at two different temperatures, the characteristic Debye temperature Θ_i, for the corresponding site can be determined. The Debye-Waller factors for the different sites at room temperature $f_i(300\ \mathrm{K})$, have been calculated from the high-temperature approximation Eq. (2). The Θ_i and $f_i(300\ \mathrm{K})$ values for all lines are given in Table IV. By making use of the estimated Debye-Waller factors at room temperature and from the measured intensities for all temperatures given in Table III, the Debye-Waller factors have been calculated. These values are plotted in Fig. 4 as a function of the measuring temperature. The dotted curves shown in Fig. 4 are the Debye functions [Eq. (1)] calculated with the appropriate Debye temperatures. It appears that the experimentally determined temperature dependence of the Debye-Waller factor for each line is reproduced fairly well by the Debye approximation in the investigated temperature range. The only deviation is found in the low-temperature region for line 5, where the value at 4 K falls significantly below the calculated Debye curve.

The sample implanted with 5×10^{14} atoms/cm^2 at 723 K has been measured at 300 and 77 K to obtain Debye temperatures from the high-temperature approximation. Although the validity of the high-temperature Debye approximation at 77 K can be contested, it has been used in the actual case to extrapolate the characteristic Debye temperatures and Debye-Waller factors for all five lines. The systematic error is estimated to $\lesssim|-3\%|$. These values are also given in Table IV.

The Debye temperatures measured for the lines 2, 3, and 4 are in satisfactory agreement with those measured for the respective lines for similar implan-

TABLE III. ^{119m}Te implanted in silicon. Intensity of lines (arbitrary units) as a function of measuring temperature.

Meas. temp. (K)	I_2	I_3	I_4	I_5
4	1.24(8)	0.52(5)	0.12(3)	0.16(4)
20	1.27(8)	0.47(5)	0.11(3)	0.22(4)
100	1.04(6)	0.45(5)	0.09(3)	0.14(3)
200	0.85(5)	0.22(4)	0.08(3)	0.08(3)
300	0.61(5)	0.13(3)	0.06(3)	0.04(2)

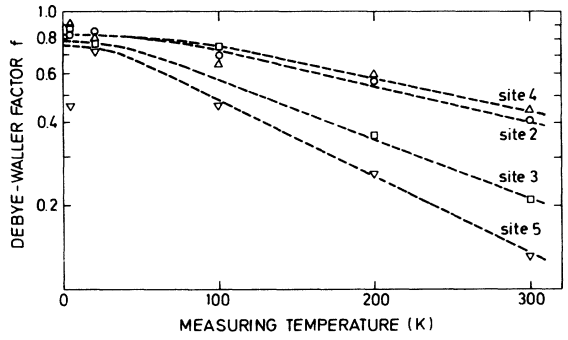

FIG. 4. Temperature dependence of the Debye-Waller factors for different sites of ^{119m}Te in silicon.

TABLE IV. Debye-Waller factors at 300 K and characteristic Debye temperatures Θ_i(K).

	f_1	Θ_1	f_2	Θ_2	f_3	Θ_3	f_4	Θ_4	f_5	Θ_5
From 300 and 4 K measurements	...	...	0.41(6)	230(20)	0.21(8)	170(25)	0.44(5)	240(30)	0.13(8)	150(20)
From 300, 200, and 100 K measurements	...	...	0.45(4)	240(15)	0.15(6)	160(15)	0.49(5)	260(20)	0.15(6)	160(15)
From 300 and 77 K measurements (see Sec. III C)	0.40(6)	230(20)	0.47(6)	250(20)	0.21(6)	175(20)	0.39(10)	230(40)	0.26(6)	200(20)
Weighted average from high-temp. data	0.40(6)	230(20)	0.46(3)	250(15)	0.18(4)	165(15)	0.47(5)	250(18)	0.21(5)	175(15)

tations of ^{119}Sb (Part I). Thus for ^{119m}Te implantations, some of the Sn atoms are found in the same defect structures (lines 2, 3, and 4) as for ^{119}Sb implantations.

D. Annealing experiments

Because of the radioactive chain ^{119m}Te(4.7 d) $\rightarrow$ ^{119}Sb(38 h) $\rightarrow$ ^{119}Sn, the annealing properties of related defects associated with both Te and Sb after an implantation of ^{119m}Te can be studied. When the implanted ^{119m}Te is in radioactive equilibrium with its decay products (this is reached $\gtrsim$60 h after the implantation), two different types of annealing experiments can be performed. If the annealing time and the measuring time following the annealing are short compared to the half life of ^{119}Sb, the measured Mössbauer γ radiation comes from decaying atoms having been annealed as Sb atoms, since most of the decaying Sb atoms were formed prior to cool down. On the other hand, if the measurement is performed after a time long compared to the Sb half life, then the γ radiation stems from atoms having been annealed as Te atoms, since most of the annealed Sb atoms have now decayed. Thus, whether the annealing properties of Sb or Te are measured in such Mössbauer experiments, is determined by the time elapsed between the cool down and measuring time.

The low-temperature data from these two types of annealing experiments are given in Table V and displayed graphically in Fig. 5 (open symbols) for a low-dose, room-temperature implantation measured at room temperature. Also plotted in Fig. 5 are the data for the lines 2 and 3 from an isochronal annealing on a high-dose, room-temperature implant (closed symbols). From Table V, it appears that while intensity changes for lines 3, 4, and 5 first occur between 750 and 850 K, first intensity changes occur at a much lower temperature (450–500 K) for line 1. In addition, the intensity changes at ~800 K may occur at slightly different temperatures for the different lines as can be seen from the graphical display. Furthermore, the annealing stage of line 3 might be dose dependent, since it seems to be different for the two samples, however, finer tempera-

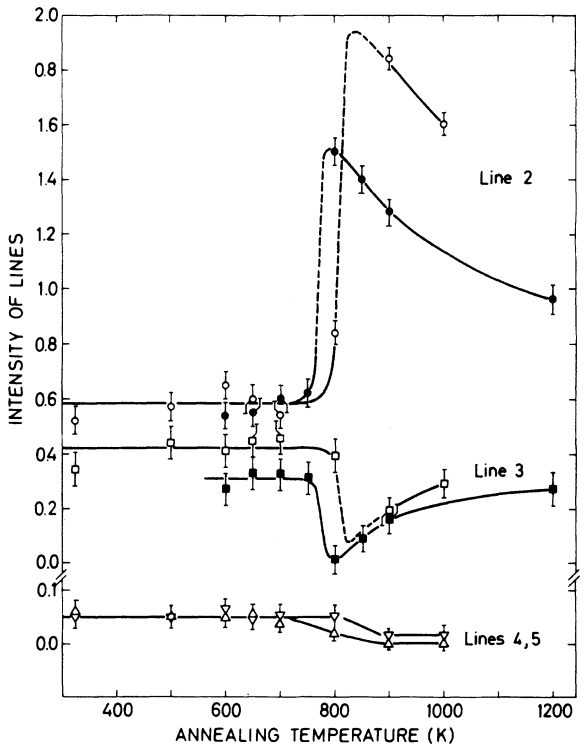

FIG. 5. Intensity of emission lines measured within 12 h after isochronal annealing (20 min) at different temperatures from samples implanted with ^{119m}Te at room temperature. The symbols represent line intensities, circles: line 2, squares: line 3, triangles on the base line: line 4, triangles on the vertex: line 5. Open and filled symbols correspond to low- and high-dose implantations, respectively.

TABLE V. Intensity of lines (arbitrary units) for isochronal annealing of ^{119m}Te implanted in silicon.

Annealing temperature (K)	I_1	I_2	I_3	I_4	I_5	$\sum_i P_i^a$	$\sum_i P_i^b$
. . . [c]	0.05(2)	0.52(5)	0.34(6)	0.06(2)	0.05(2)	0.80	0.89
473	0.05(2)	0.57(5)	0.44(6)	0.05(2)	0.05(2)	0.96	1.03
523	0.02(2)	0.63(5)	0.39(6)	0.06(2)	0.04(2)	0.89	0.96
573	0.02(2)	0.65(5)	0.41(6)	0.05(2)	0.06(2)	0.93	1.03
623	0.0	0.60(5)	0.45(6)	0.05(2)	0.04(2)	0.93	1.00
673	0.0	0.54(5)	0.47(6)	0.04(2)	0.05(2)	0.93	1.03
773	0.0	0.84(4)	0.39(6)	0.02(1)	0.05(2)	0.98	1.05
873	0.0	1.84(4)	0.19(5)	0.0	0.01(1)	1.16	1.05
973	0.05(2)	1.60(4)	0.29(5)	0.0	0.02(1)	1.21	1.05
973[c]	0.08(3)	0.83(5)	0.53(6)	0.03(1)	0.06(2)	1.21	0.91

[a]Calculated with $f_1=0.4$, $f_2=0.46$, $f_3=0.18$, $f_4=0.47$, $f_5=0.21$.
[b]Calculated with $f_1=0.4$, $f_2=0.46$, $f_3=0.18/0.44$, $f_4=0.47$, $f_5=0.1$.
[c]Measurements performed $\gtrsim$200 h after implantation or annealing (annealed as Te). Other spectra measured within 12 h after annealing (annealed as Sb), annealing time 20 min.

ture steps and better statistical accuracy would be needed to prove this in detail. As the temperature is increased above ~800 K, the intensity of line 2 is observed to decrease while the intensity of line 3 increases. The data obtained after annealing at ~1000 K and after a long delay indicates that for Te atoms, hardly any effect of the annealing is observed apart from slight increases of the intensities of the lines 2 and 3.

Other annealing experiments at higher temperatures were performed on a high-dose, room-temperature-implanted Si crystal. The results from this annealing series are given in Table VI. The intensity of line 2 shows similar decrease through this annealing series from ~900 to 1400 K as found in the other annealing series between 800 and 1200 K (Fig. 5). This is also the case for the intensity of line 3 after ~900 and 1200 K annealings. However, after the 1400 K annealing, the line 3 intensity drops to zero both for annealed Sb and Te. Thus, after the 1400 K annealing, no atoms are found in the structure assigned to line 3. From the constancy of the intensity of line 2, it can be concluded that the line 3 atoms do not migrate to substitutional positions but primarily contribute to the intensity of line 4. (The intensity of line 4 is seen to increase after the high-temperature annealing both for annealings associated with Te and Sb atoms.) The intensity of line 5 shows an oscillating behavior. For anneals as Sb atoms, the intensity of this line drops to nearly zero but for anneals as Te atoms, the intensity shows an increase after the ~1200 K annealing.

TABLE VI. Intensity of lines (arbitrary units) for high-temperature isochronal annealing experiments on ^{119m}Te implanted silicon.

Anneal. temp.(K)	I_2	I_3	I_4	I_5	$\sum_i P_i^a$	$\sum_i P_i^b$
. . . [c]	0.51(5)	0.16(4)	0.04(2)	0.02(1)	0.85	0.88
873[d]	1.12(6)	0.04(2)	0.02(1)	<0.01	1.07	0.99
1173[d]	1.00(6)	0.12(2)	0.14(3)	0.04(2)	1.29	1.18
1173[c]	0.52(5)	0.10(3)	0.12(3)	0.10(3)	0.94	0.99
1373[d]	1.00(5)	<0.01	0.20(4)	<0.01	1.05	0.99
1373[c]	0.52(5)	<0.01	0.18(4)	0.10(3)	0.80	0.96

[a]See Table V, footnotes b and c.
[b]See Table V, footnotes b and c.
[c]Annealed as Te atoms.
[d]Annealed as Sb atoms.

E. Postimplantations

In order to study whether the implantation of Sb and Sn atoms together with the Te activity in the Si crystals had any influence on the intensities of the different lines, postimplantations of stable Sb and Sn have been performed in ^{119m}Te implanted crystals. Figure 6 shows the results from two postimplantations. In one of the experiments (implanted Te dose: 5×10^{14} atoms/cm^2 at ~700 K, postimplanted Sb dose: 5×10^{14} atoms/cm^2 at ~700 K), both measurements at room temperature (indicated by squares in Fig. 6) and at liquid-nitrogen temperature (indicated by circles in Fig. 6) have been performed. These two sets of data have been normalized to each other for the graphical representations by means of the ratios of the Debye-Waller factors given in Table IV. In the other experiment (implanted ^{119m}Te dose: 10^{12}–10^{13} atoms/cm^2 at ~700 K, postimplanted Sn dose: 5×10^{14} atoms/cm^2 at ~700 K), only room-temperature measurements have been performed (indicated by triangles in Fig. 6). The intensities from this implantation have been normalized to the first measurement before the postimplantation. In both experiments, one or two lines showed only low intensities, these lines have therefore been omitted in the figure. The measurements immediately after the postimplantations have been performed in a time short compared to the ^{119}Sb half life, this means that the γ radiation stems from atoms which were Sb atoms during the postimplantation (Sec. III C).

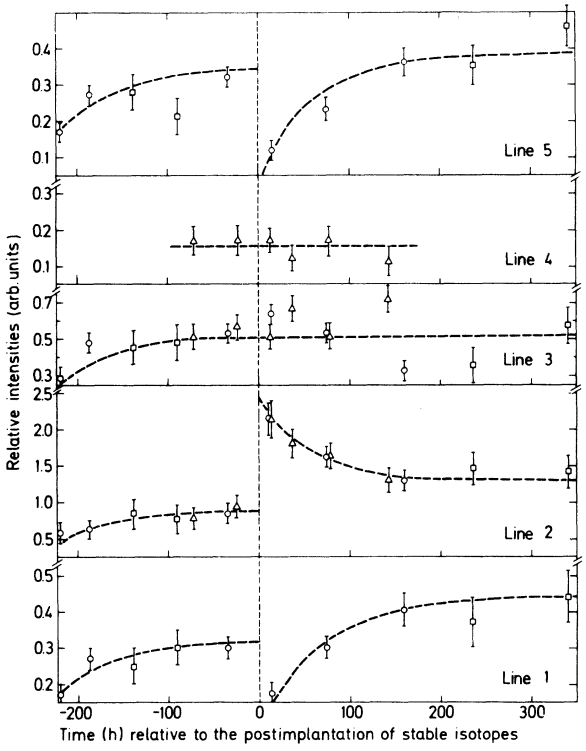

FIG. 6. Intensities of lines in Mössbauer spectra of implanted ^{119m}Te in silicon. The spectra have been measured at different times relative to a postimplantation of stable isotopes into the sample. The curves in the figure represent the different time dependences of the intensity of lines as expected from the nuclear decay chain ^{119m}Te ($4.7d$) $\rightarrow$ ^{119}Sb $\rightarrow$ ^{119}Sn (see text). Measurements at liquid-nitrogen temperature (and room temperature) are indicated by circles (and squares) for one series of experiments and have been normalized to each other. Measurements at 77 K on stable Sn postimplanted sample are indicated by triangles.

Drastic changes are observed in the intensities of lines 1, 2, and 5 immediately after the postimplantation. The intensity of lines 1 and 5 drops to approximately zero and then grows in accordance with the radioactive decay laws for the growth of a short-lived daughter (^{119}Sb) from a long-lived mother (^{119m}Te). The intensity of line 2 reaches its highest value immediately after the postimplantation and decays afterwards exponentially in time with the mean life of ^{119}Sb. All three sets of data have been fitted with functions of the form $I = A \exp(-t/\tau_{Sb}) + B$, where A and B are constants and τ_{Sb} is the mean life of ^{119}Sb($\tau_{Sb} = 54.8$ h). No significant changes are observed in the intensity of lines 3 and 4 after the postimplantations. (In the time immediately after the original ^{119m}Te implantation, a weak, exponential growth of the intensities of all lines is observed, which is in accordance with the growing in of the ^{119}Sb from the ^{119m}Te because only minor amounts of ^{119}Sb were implanted together with the ^{119m}Te activity.)

It is not expected that the creation of spikes during the postimplantations will result in any defect rearrangement.[19] It is more likely that the observed intensity variations are due to atomic collisions and the results indeed indicate that the Sb atoms which originate from decaying Te atoms, during the postimplantation behave as if they were newly implanted. The number of displaced atoms per incoming ion has been estimated to be approximately 3000 for 40-keV Sb ions implanted in Si.[20] For an implanted dose of 5×10^{14} atoms/cm^2, all atoms in the implanted layer will then undergo elastic collisions and will be displaced from their positions. The radioactive ^{119}Sb atoms in the layer (which originally stemmed from the decay of ^{119m}Te) during postimplantations are no longer influenced by their origin and will be located at positions which are typical for implanted Sb. These positions are known to be associated with lines 2, 3, and 4 and not those associated with lines 1 and 5. In a short time after the postimplantation the intensity of lines 1 and 5 should therefore be zero and the intensity of lines 2, 3, and 4 should be unchanged if the Sn defects assigned to these lines are the same for Sb and Te. These expectations are in good agreement with the experimental findings. The intensities

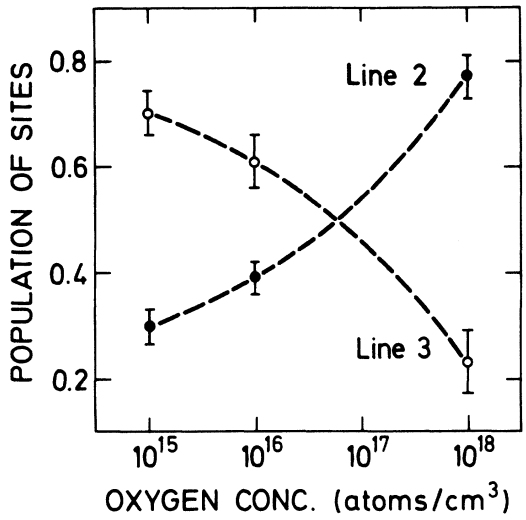

FIG. 7. Dependence of sites 2 (filled circles) and sites 3 (open circles) on the oxygen content of the implanted silicon samples.

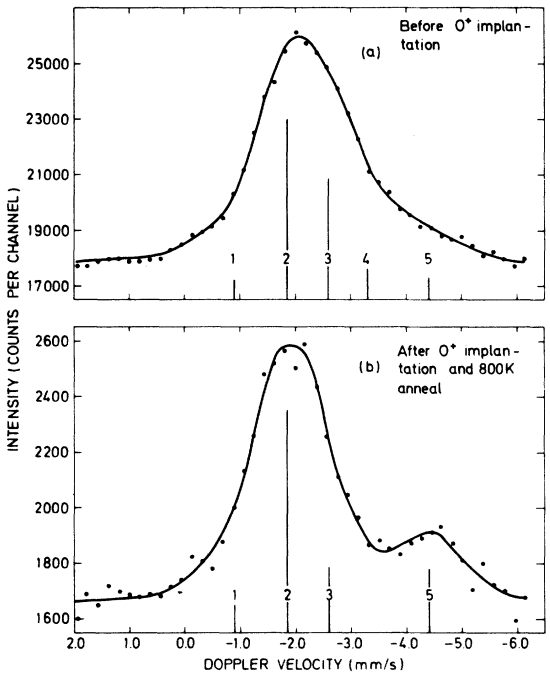

FIG. 8. Mössbauer spectra of ^{119m}Te in silicon before (a) and after a postimplantation of oxygen followed by an annealing at ~800 K (b). The curves represent fits to the data in terms of emission lines as indicated by the bars.

of lines 3 and 4 are nearly constant. From the increase in the intensity of line 2, it can be concluded that those fractions of radioactive Sb atoms that earlier occupied positions 1 and 5, occupy substitutional positions (line 2) after the postimplantation.

As ^{119m}Te decays to ^{119}Sb, those lines that are typical for implanted ^{119m}Te are again seen as they grow in exponentially with the mean life of ^{119}Sb.

The data indicate that the intensities reached by lines 1, 2, and 5 a long time after the postimplantation are somewhat higher than before. A similar effect is observed in the annealing experiments, and might be due to small variations in the Debye-Waller factors of some of the sites, which could possibly be caused by slight rearrangements of the defect structures (for example, the agglomeration of larger defects at higher annealing temperatures).

F. The influence of the oxygen content of the silicon crystals

Preliminary studies of ^{119m}Te implanted in silicon showed that the intensity of the different lines changed in a nonsystematic way when silicon crystals of different origins were used. In order to examine this in more detail, low-dose ($<10^{13}$ atoms/cm^2), room-temperature implantations of ^{119m}Te in n-type silicon crystals with different oxygen concentrations have been performed. As the intensities of lines 1, 4, and 5 are relatively low in all these implantations, the dependence of these lines on the oxygen content of the host crystal is not conclusive. The measured intensities have been converted to the fractions of sites as described in Sec. III B, these fractions of sites are plotted in Fig. 7 versus the approximate oxygen concentration of the Si crystals on a logarithmic scale. The data indicate a distinct dependence of the fractions of the sites 2 and 3 on the oxygen content. For crystals with high oxygen concentration, most of the implanted atoms end up in substitutional positions.

TABLE VII. Effect of postimplantation of oxygen (3×10^{14} atoms/cm^2 at 25 keV, RT) on a ^{119m}Te implanted silicon crystal (dose $\lesssim10^{13}$ atoms/cm^2, RT, CZ grown). The sample was annealed at 773 K for 30 min after the oxygen implantation. The following Debye-Waller factors have been used to estimate the population of sites: $f_1=0.40$, $f_2=0.46$, $f_3=0.18/0.44$, $f_4=0.47$, $f_5=0.13$.

	I_1	P_1	I_2	P_2	I_3	P_3	I_4	P_4	I_5	P_5	f_3	$\sum_i P_i$
As implanted	0.03(2)	0.02	0.44(4)	0.29	0.29(4)	0.49	0.09(3)	0.06	0.06(2)	0.14	0.18	1.0(1)
^{16}O implanted and annealed	0.08(3)	0.06	0.63(4)	0.56	0.19(3)	0.13	...	...	0.18(3)	0.41	0.44	1.1(1)

A similar effect of oxygen has been observed for an implantation of oxygen after the original radioactive Te implantation. The postimplantation of oxygen (25 keV, peak concentration 1×10^{20} atoms/cm^3) was followed by a 20-min annealing at ~800 K. No changes of the spectra were observed before the annealing. The spectra measured before and after (delay time more than 60 h) the postimplantation and the annealing are shown in Fig. 8, spectra *a* and *b*, respectively, and the results are summarized in Table VII. From the analysis, line 3 decreases, while line 2 increases after the oxygen implantation and annealing. Lines 4 and 5 change similarly.

IV. DISCUSSION

A. Spectral decomposition

Several Mössbauer isotopes implanted in group-IV elements with diamond structure (C,Si,Ge,α-Sn) show a striking similarity in their spectra, namely, that two separate (groups of) lines are observed. Such spectra were measured for the Mössbauer transition of ^{129}Te,[6,21] ^{125}Te,[10,22] ^{119}Sn,[11,12] ^{57}Fe,[23–27] and ^{129}Xe.[22] The values of most isomer shifts for these two groups display the same systematic dependence on parameters of the group-IV host materials, e.g., the nearest-neighbor distance. Linear dependences (with distinctly different slopes for the two groups of lines) on this parameter are observed for the electron densities at the nuclei of the impurity atoms. However, no unique interpretation has been given. For ^{57}Fe, there has recently been found direct evidence for an interpretation of these two groups of lines in terms of a quadrupole split double.[28,29]

In an earlier report on ^{119m}Te implanted in group-IV elements,[7] an attempt to analyze the Mössbauer spectra by only two lines was made. The dominating, broadened line was attributed to substitutional or nearly substitutional sites and a smaller broadened line was attributed to interstitial or nearly interstitial sites. As the experimental data became more and more comprehensive, it became clear that it was not possible to fit all data consistently with only two broadened lines. It was found necessary to introduce five individual, nearly unbroadened emission lines to fit all the existing data of ^{119m}Te implanted in both Si and the other group-IV elements. Much help in establishing the existence of these five lines was obtained from the Mössbauer studies of ^{119m}Sn (Refs. 13, 14) and ^{119}Sb implanted in Si (see Part I). For ^{119m}Sn implanted in Si at elevated temperature, only one line is observed in the Mössbauer spectra. This line is known to originate from substitutional Sn atoms and is easily identified to be present also in the spectra of ^{119m}Te implanted in Si. When ^{119}Sb is implanted in Si, two more lines are observed, both with higher isomer shifts. These two lines are also observed in the ^{119m}Te implantations (lines 3 and 4). Among these two lines, line 3 has been easiest to identify. Its annealing behavior, the temperature dependence of the corresponding Debye-Waller factor, the intensity dependence on the oxygen concentration of the crystals are all very different from what is observed for line 2, which shows that it is an independent line and cannot be accounted for by a broadening of line 2. Finally the postimplantation experiment gives direct evidence that this line is the same line as observed in the ^{119}Sb implantations.

The observed temperature dependence of the Debye-Waller factor of line 4 is quite different from the one observed for line 3 (and line 5) which demonstrates that this is also an independent line and cannot be accounted for by a broadening of line 3. Furthermore this line is comparably well resolved for Sb implantations (Part I). Again, the constancy of the intensity during the postimplantations reveals that the same line occurs in the ^{119}Sb implanted samples.

The difference in isomer shifts between line 5 and line 4 (1.1 mm/s) is larger than the difference between line 3 and line 4 (0.7 mm/s). This fact (together with a slightly higher intensity for line 5) makes it relatively easy to identify line 5 spectroscopically. The temperature dependence of the Debye-Waller factor of line 5 is very different from that observed for line 4, and in addition, the intensity of the line shows a dependence on the oxygen concentration of the crystals different from those of lines 3 and 4. The postimplantation experiments demonstrate that line 5 is typical for ^{119m}Te implanted in Si and not for the ^{119}Sb implantations.

The most difficult line to identify was line 1. But the observation of an anneal temperature different from that for lines 3, 4, and 5 shows that it is an independent line. This is also supported by the postimplantation experiments, which distinguish this line clearly from line 2. The postimplantation experiments demonstrate that this line is typical for ^{119m}Te implantations in agreement with the results from the ^{119}Sb experiments (Part I).

As discussed in Part I, a possible influence of the radioactive decay of implanted impurity atoms on the Mössbauer spectra has to be considered. The electron-capture decay of ^{119m}Te is quite similar to the radioactive decay of ^{119}Sb and what has been said about nonequilibrium charge states of the decaying ^{119}Sb (Part I) atoms can immediately be applied to the decaying ^{119m}Te. The recoil energy transferred to the decaying ^{119m}Te atoms is higher than in the case of ^{119}Sb ($\gtrsim$8.4 eV for 90%, $\approx$20 eV for 10% of the decays) but still smaller than the expected displacement energies[15] for most decays (see discussion in Part I). Thus also in this case no permanent displacement seems likely to precede the nuclear decay for about 90% of the atoms. However, for a fraction

of ~10% of the Te atoms a displacement from the original positions occupied in the implantation is possible. The relevant electronic structure for the interpretation of the Mössbauer spectra is that of Sn. As discussed in Part I, electronic relaxation and possibly lattice relaxation occur in the course of the radioactive decays. On the other hand, since Te implantations produce Sn-defect structures different from those of Sb implantations, undoubtedly some characteristics of the original structures are maintained after the radioactive decay. Furthermore, no other impurity sites besides the substitutional sites have been found for Sn implantation in silicon[13,14] in contrast to what is observed for Sb (cf. Part I) and Te implantations.

B. Site assignment for line 2

From the measured isomer shift and Debye temperature of line 2, this line can be identified to be the same as observed for ^{119m}Sn implanted in silicon,[13,14] and the same line as line 2 observed for ^{119}Sb implanted in silicon (see Part I). This line is known to originate from Sn atoms on undisturbed substitutional sites. (For a thorough discussion of line 2, the reader is referred to Refs. 13, 14, 30, 31, and to Part I of this paper.)

C. Site assignment for line 3

The most intense line next to the substitutional line in all the ^{119m}Te implantations is line 3. From the isomer shift, Debye temperature and annealing behavior, it can be concluded that this is the same as line 3 observed for ^{119}Sb implanted in silicon. In Part I of this paper it was shown that a consistent interpretation of this line could be obtained if one assumes that the line originates from Sn atoms associated with vacancies. Reasonable interpretations were found for the measured isomer shift and Debye temperature using simple calculations of these parameters from a model assuming substitutional Sn atoms with adjacent vacancies. Qualitatively, the impurity atoms are concluded to have a dangling bond, but no definite conclusion on the importance of electronic or lattice relaxations could be drawn due to the simplicity of the theoretical approach. Because of the relatively high annealing temperature for this defect, "simple" isolated parent defects such as the Sb monovacancy could, however, be excluded. Instead, a larger defect structure, probably a cluster of vacancies (at least two), causing considerable lattice relaxation, has to be assumed, in which the Sb atom resides in a "substitutional" position with one nearest-neighbor vacancy. The additional experimental information on line 3 obtained from the ^{119m}Te implantations is found to be in agreement with those from the ^{119}Sb implantations and thus supports the above model for a vacancy associated impurity.

The annealing behavior of line 3 and also of the substitutional line 2 consists of three regions as displayed in Fig. 5. The drastic changes in the relative intensities of the two lines take place in the temperature range between 700 and 800 K, which is typical for the dissociations of large defect clusters.[20] However, only the structures containing Sb atoms anneal in this temperature range; the same structures containing Te are hardly influenced. A heat treatment at 1300–1400 K is needed in order to influence Te atoms in these structures. The stability of the defect structures containing Sb suggest that all structures are clusters composed of several defects. The annealing behavior of the Sb atoms from the radioactive decay of Te is in agreement with the results from direct implantations of ^{119}Sb (see Part I).

The decrease of the substitutional line and the corresponding increase in the intensity of a line 3′ (with the same isomer shift but a higher Debye temperature than line 3) is observed at higher anneal temperatures for Sb and is probably associated with the formation of dislocation loops. In electron-microscopy studies of room-temperature-implanted silicon,[32] a high density of dislocation loops is found after the annealing of damage clusters during implantation. A decoration of such dislocation loops by heavy impurity atoms, including Sb, has been proposed by Gibbons.[33] It is not unlikely that such a decoration could result in an electronic configuration of the impurity atom with a dangling bond. The observation that line 3′ disappears after a ~1400 K annealing both when the line stems from annealed Sb and Te seems to exclude that the observed effect is due to a diffusion of Sb and Te atoms to the surface of the crystal.

The values of the sums $\sum_i P_i = \sum_i I_i/f_i$, calculated for the annealing series are included in Tables V and VI. This sum should be a constant, presuming the ratios of the f factors are correct, and is thus an independent check of the f-factor ratios. In Tables V and VI, the sums are given as calculated with the weighted mean value f factors from Table IV (indicated by $\sum_i P_i^a$). It appears that there is a step in the sum after ~900 K annealings and that the sum in Table VI oscillates in value (the value is lower for a delayed measurement than for a measurement immediately after the annealing). The oscillating behavior suggests that f_5 might be too high and the jump after ~900 K annealing suggests that f_3 might change in value at this annealing step. To allow for this, the f_3 and f_5 factors have been varied. It turns out that almost constant sums can be obtained if f_3 is assumed to change in value after ~900 K annealing from $f_3 = 0.18$ to 0.44 and if f_5 is lowered to $f_5 = 0.1$. The resulting sums are also given in Tables V and VI (indicated by $\sum_i P_i^b$). It is not surprising that a

change in f factor for line 3 at ~900 K has to be assumed in order to get consistent results, because at this temperature the possible origin of this line is changed from an Sb vacancy cluster (line 3) to a Sb-decorated dislocation loop (line 3'), and although the electronic configuration (as deduced from the isomer shift) is similar in the two structures, the dynamics of the motion of the Sb atoms need not be the same. The change in f factor for line 3 after an annealing at ~900 K is the same as found for implantations of Sb (cf. Part I).

The assignment of site 3 to a (nearly) substitutional Te atom associated with vacancies is consistent with the observed correlation between the oxygen concentration in the silicon crystals and the occurrence of this site and the substitutional site. Oxygen is known to be an efficient trap for vacancies.[34] The decrease in line 3 with increasing oxygen content of the samples can thus be explained to be due to a competition between Te and O to trap vacancies.

The following simplified picture can given an idea of the number of atoms involved in the processes. An implanted dose of 1×10^{13} Te atoms/cm^2 in silicon corresponds to an averaged concentration of 3×10^{18} Te atoms/cm^3. A cubic box with an edge length of 150 Å will then contain approximately 10 Te atoms and approximately 10^5 Si atoms. Out of these 10 Te atoms, approximately 5 will be in substitutional sites and approximately 5 in sites 3 (and approximately 1 in either of the sites 4 or 5). For a silicon crystal with low oxygen concentration (~10^{15} atoms/cm^3), no oxygen will on the average be contained in this box. On the other hand, for a silicon crystal with a high oxygen content (~2×10^{18} O atoms/cm^3), around 10 O atoms will be contained in this box. Because of the affinity of oxygen to trap vacancies, possible vacancy candidates for the creation of line 3 will be trapped by these O atoms and thus more Te atoms will occupy substitutional sites. A postimplantation of oxygen in a ^{119m}Te implanted Si crystal to a dose of 3×10^{14} atoms/cm^2 at 25 keV did not reduce the intensity of line 3, but followed by a ~800 K heat treatment in 20 min, an appreciable reduction was observed. The projected range of 25-keV O ions in Si is ~600 Å with a projected standard deviation of ~200 Å, which means, when compared to the projected range of 60-keV Te ions in Si of ~300 Å with a projected standard deviation of 100 Å, that nearly all the O ions are stopped in a deeper layer than the implanted Te layer. Thus, a postimplantation of 25-keV O ions alone is not expected to alter the intensities of the lines, in agreement with the experimental finding. The observed reduction in the intensity of line 3 after the 800 K heat treatment cannot be due to a thermal dissociation process, since the annealing studies show that site 3 when associated to Te does not break up even after a ~1200 K heat treatment. On the other hand, oxygen is mobile in Si at ~800 K.[35] Thus, the most probable explanation for the observed reduction is that during the heating process, the O atoms move freely around in the lattice and are capable of being trapped at vacancies. Because of the high concentration of oxygen (a rough estimate gives about 50 O atoms in the above mentioned box), this process can easily result in an appreciable reduction of the Te-vacancy structures, giving rise to an increase in the number of substitutional Te atoms. In this model, the affinity of oxygen to trap vacancies must be larger than that of Te, otherwise the Te-vacancy defect structure would not break up.

D. Site assignment for line 1

The experimental information about line 1 is not as comprehensive as the information about line 3. This is mainly due to the low intensity of this line found in most of the implantations, which is just on the limit of what is experimentally observable. However, conclusions can be drawn from the data. Valuable information is obtained from the annealing behavior of this line. Although the accuracy of the annealing data for this line is relatively poor due to the low intensity, the data indicate, however, that the intensity is reduced during a heat treatment at ~500 K if the defect is associated with Sb. No reduction of the intensity of the line is observed when the defect is associated with Te, not even after a ~1000 K heat treatment. The relatively low annealing temperature for the Sb associated site indicates that the site could be correlated to a rather simple type of defect, for example, a divacancy.

Observations of Sn-vacancy[36,37] and Sb-vacancy defects[38] have been reported previously. Recently, Watkins[39] found a tin-divacancy defect by electron-paramagnetic-resonance measurements on electron irradiated silicon containing Sn impurities. He proposed a model in which the Sn-impurity atom resides between two vacant lattice sites in the ⟨111⟩ direction, this means in an interstitial position in the center of a divacancylike defect. In this position the Sn atom is equidistant from six silicon atoms, which form a distorted octahedron around the tin atom. The outer electronic configuration of the tin atom in this position was proposed to be that of hybridized $5s\,5p\,5d$ orbitals to form bonds with all six nearest neighbors.

An estimate of the isomer shift expected for tin impurity atoms with this electronic configuration can be obtained from known isomer shifts of tin compounds with similar electronic configurations. In stannic sulphide, SnS_2, the tin atom is expected to have this particular electronic configuration with the six hybrid orbitals directed towards the spires of an octahedron. The isomer shift has been measured to

be 1.11 mm/s,[40] in reasonable agreement with the isomer shift of 0.92 ± 0.08 found for site 1. No strong quadrupole splitting of the line is expected since all the orbitals are bonding, which results in no unbalanced p electrons. The Sn-divacancy complex was found to anneal at a temperature of ~500 K, which agrees with the annealing temperature of site 1.

Although the preceding discussion cannot be taken as proof that site 1 is the same type of defect complex as observed by Watkins, the concordant experimental observations make it, however, highly probable.

E. Site assignment for lines 4 and 5

In most implantations, these two lines appear with low intensities: typically 10–15% of the implanted ^{119m}Te atoms occupy the sites 4 and 5. The question may arise whether the lines originate from two sites with different chemical surroundings giving rise to two different isomer shifts or from a single site with an electric quadrupole interaction. The latter possibility can be excluded because only line 4 is observed in the Sb implantations, and thus no indications are found for a correlation of lines 4 and 5. Also the marked difference in the temperature dependence of the intensities of the two lines in the temperature range from 4 to 300 K (Fig. 3) together with a slight difference in the annealing temperature supports the exclusion of this possibility.

The outstanding features of these two lines are firstly the isomer shifts, which correspond to high s-electron densities at the Sn nuclei, and secondly the dependence of these isomer shifts on the nearest-neighbor distance in group-IV hosts.[11] For both sites this dependence is found to be linear, following almost parallel lines for the two sites. The straight lines appear to rise steeply with decreasing nearest-neighbor distance, opposite to what has been found for the substitutional lines. These observations suggest that the interaction of these atoms with their surrounding must be quite different from the chemical bonding observed for the substitutional site. The dependence of the electron density on the nearest-neighbor distance has been attributed to compressional effects.[11] The measured isomer shifts belong to a range corresponding to electronic configurations of the valence electrons characteristic for atomic Sn[$5s^2 5p^2$, $\delta = 3.2$ mm/s (Ref. 41)] or Sn^{2+}[$5s^2$, $\delta \simeq 4.8$ mm/s (Ref. 42)]. However, because compression effects may play a considerable role, even if the electronic structure of the impurity atoms would be adequately described by one of these configurations, the measured isomer shift might be shifted to a higher value.

For the two largest interstitial sites in the diamond lattice, the impurity atoms are expected to be in nonbonding configurations. This means probably in an atomic electronic configuration. These two sites, the tetrahedral- and the hexagonal-interstitial site, are both highly symmetrical with four nearest neighbors at distances of $0.433a_0$ and six nearest neighbors at distances of $0.415a_0$, respectively (a_0 is the lattice constant). According to Weiser,[43] small ions should prefer the hexagonal site, while larger ions should prefer the tetrahedral site. Following this, the large Te atoms will then most likely occupy the tetrahedral interstitial site. In neither of these sites are the Te atoms supposed to disrupt the covalent bonds between the neighbor host atoms, although they might distort them. Large compression effects are therefore expected. Since the lattice cell volume decreases, when going from α-Sn to Ge to Si to diamond, the s-electron density at the Sn nucleus will increase because of the enhanced compression. This results in higher isomer shifts. Even for a Sn atom residing in the tetrahedral interstitial site of α-Sn, a compression is expected. (The atomic radius of Sn, $R_{at.} = 1.62$ Å, is larger than the radius of the interstitial cavity in α-Sn, $R_{tet} = 1.40$ Å, giving a volume excess of ~60%.) This implies that the isomer shift of the Sn atom in this site in α-Sn should be larger than the isomer shift of atomic tin. From these considerations it emerges that both lines 4 and 5 might originate from impurity atoms in tetrahedral (or hexagonal) interstitial sites. The isomer shift for line 5 in α-tin, $\delta = 4.1$ mm/s,[12] is rather high, however, when compared to the value for the atomic configuration. The isomer shift of line 4, on the other hand, when extrapolated to α-Sn, $\delta = -3.1$ mm/s,[12] is slightly below the value of atomic Sn. It might be speculated, that a vacancy nearby this interstitial atom would relax the compression, resulting in a smaller isomer shift for this system. On the basis of this, line 4 could be interpreted as arising from some kind of vacancy-interstitial Sn defects. This interpretation is not in conflict with the observed decrease in the intensity of the line and the corresponding increase in the intensity of line 5 after the oxygen postimplantation and the heat treatment, if a mechanism similar to the one responsible for the observed reduction in the intensity of line 3 is assumed. Then the migrating oxygen atoms capture the vacancies nearby the interstitial impurity atoms which results in a decrease in the intensity of line 4 and, if the remaining impurity complex yields a line-5 spectrum, a corresponding increase in the intensity of line 5. However, as will be discussed in the following, this interpretation of the two lines as being due to single interstitial impurities in the host lattice is in conflict with the second outstanding feature of these lines, namely, the large difference in their Debye-Waller factors.

The temperature dependences of the Debye-Waller factors for the two sites as displayed in Fig. 4, are

found to be fitted satisfactorily with Debye curves in the temperature range from 4 to 300 K, except for the low-temperature measurements on line 5. Between 20 and 4 K, the intensity of this line drops significantly. This seems to be a real effect and not due, for example, to the applied fitting procedure as no changes in the intensities of the remaining lines are seen in this temperature region. However, the intensity at 20 K might be slightly too high, so that all low-temperature data appear to fall below the Debye curve. This corresponds to a shift in the frequencies of vibrations of the impurity atom towards lower frequencies. This indicates that the Debye model is inadequate to explain the temperature dependence. The characteristic Debye temperatures and Debye-Waller factors extracted from the temperature dependences of the intensities are found to be quite different for sites 4 and 5.

At any rate, although interpretations based on a simple (and inadequate) Debye model have to be considered with reservations, it is evident that the Debye-Waller factor of site 4 is much larger than the Debye-Waller factor of site 5 at room temperature. This result is difficult to incorporate into the picture of the two lines given in the preceding discussion. A vacancy nearby an atom in a lattice (substitutional interstitial atom) will result in an increase in the mean-square vibrational amplitude of the atom at least in the direction of the vacancy, giving rise to a smaller Debye-Waller factor. According to this, in particular, the interpretation of line 4 as originating from a vacancy-interstitial Sn defect seems doubtful. A more complicated structure probably has to be introduced to account for the observed behavior. This is also demanded by the annealing experiments (Table VI), where an increase in intensity of this line is observed at high temperatures indicating that the line might stem from an agglomeration of defects. The same behavior has been observed in the annealing experiments of implanted ^{119}Sb. The Sn-impurity atoms are still expected to reside in an interstitial-like position because of the (nearly atomic) s-electron density at the Sn nucleus and because of the observed dependence of the isomer shift on the nearest-neighbor distance of the host. However, some weak bonding to nearest-neighbor atoms might exist. This is not unlikely for Sn atoms in an interstitial agglomerate. The large Debye temperature and the dependence of the isomer shift on the nearest-neighbor distance in group-IV elements may then be explained by compressional effects.

A correlation between the oxygen concentration in the crystal and the concentration of these defect agglomerates can be expected even if the defect agglomerates are of interstitial nature. Brelot[44] has shown that the interaction of intrinsic interstitials with oxygen is far from being negligible. The observed reduction of these defect agglomerates at high oxygen concentration can be due to a trapping of intrinsic interstitials by oxygen. As a consequence the Te atoms should be contained in oxygen defect complexes. This interpretation can consistently explain the experimental findings about lines 4 and 5. Since Te and O are isovalent, an incorporation of the Te valence electrons similar to the oxygen electrons is likely to occur. Oxygen is known to form families of vacancy-defect structures including several oxygen atoms and vacancies.[34] In all these structures, the local electronic structure of the oxygen atoms has been concluded to be very similar.[34] The oxygen atoms in these vacancy complexes form bent Si–O–Si bonds. If a similar position and similar bonds to the two nearest Si atoms are assumed for the Te impurity atoms in these structures, then the electronic configuration of Sn atoms in these sites will most likely be close to $5s^2$. The larger Te atoms in comparison to the O atoms may cause a slightly different lattice position for the Te atoms. However, provided that the defect structure contains a sufficient number of adjacent vacancies, the replacement of an O atom by a Te atom seems possible. The f factor of the Sn atoms in this configuration should be lower than for a substitutional site due to the presence of adjacent vacancies and the relatively weak bonds to only two Si neighbor atoms. These qualitative considerations on the electronic configuration and the f factor for Sn in an oxygen vacancy complex are found to be basically in agreement with the experimental results on line 5. The electron density at the nucleus is slightly higher than for a $5s^2$ configuration (as expected in the presence of compressional effects). The low f factor is probably due to large vibrational amplitudes in the direction of adjacent vacancies. The increase of this line after the implantation of oxygen and an annealing at ~800 K corresponds to a decrease of lines 3 and 4 and can thus be explained as the result of the trapping of the interstitial Te atoms of line 4 in the oxygen vacancy complexes. That no substantial trapping of substitutional or vacancy associated substitutional sites by these complexes is observed is probably due to the relatively larger stability of the impurity atoms in these sites.

In a Mössbauer study on implanted ^{129}Te in group-IV elements, utilizing the 28-keV Mössbauer transition of ^{129}I, Hafemeister and de Waard[6] have reported a line which in many respects resembles line 5 observed in the present investigation. In these Mössbauer experiments, two slightly broadened lines were observed with approximately equal intensities. The isomer shift of one of the lines corresponds to a very high s-electron density at the ^{129}I nucleus and displayed a dependence on the nearest-neighbor distance of the host similar to the dependence observed for line 5. By a similar argumentation as given here, Hafemeister and de Waard proposed that this site might be the tetrahedral interstitial site. The second

line observed could be attributed to substitutional ^{129}I, for this site the s-electron density at the ^{129}I nucleus decreased with decreasing nearest-neighbor distance of the group-IV hosts. The equal intensities of both lines for ^{129m}Te implantations are definitely different from the results for ^{119m}Te. The origin of this difference is not obvious, however, since in channeling investigations of Te implanted silicon no nonsubstitutional fraction has been located in the tetrahedral or hexagonal interstitial sites from channeling experiments along major axes,[4–6] this supports the interpretation of line 5 as being similar to an oxygen vacancy complex. On the other hand, in the electron capture (EC) decay chain an annealing of Te defects may occur when these contain Sb or Sn atoms. However, no indication of such processes is found in the present experiments for sufficiently low temperatures (77 or 300 K) (cf. Figs. 3 and 7). Alternatively, effects correlated to the β decay of ^{129m}Te to ^{129}I might be of importance, especially the relatively high recoil energy transmitted to the daughter nucleus (estimated to be ~15 eV) could alter the distribution of ^{129}I atoms as compared to the implanted ^{129m}Te atoms.

V. CONCLUSION

Mössbauer spectra of the 24-keV transition of ^{119}Sn from implantations of ^{119m}Te in silicon have been decomposed into independent lines corresponding to different defects associated with the Sn atoms in the host lattice. A consistent interpretation of various experiments has been obtained in terms of the following qualitative models for the Sn atoms in these defects:

Line 1 is interpreted to originate from an interstitial position where the Sn atoms are located in the center of a divacancy with hybridized $5s5p^35d^2$ bonds to six neighboring silicon atoms. This defect anneals at ~500 K.

Line 2 stems from Sn atoms on undisturbed substitutional sites. The Sn atoms form $5s5p^3$ hybrid bonds to the four nearest neighbors (more precisely the electronic configuration can be described as $s^{1.6}p^{2.4}$ due to a rearrangement of the Sn valence electrons according to the character of the host bonds[14]).

Line 3 is concluded to be due to (nearly) substitutional Sn atoms in a vacancy associated defect structure with basically one dangling bond to adjacent vacancies. The electronic structure of the Sn atoms is characterized by a redistribution of the electronic configuration towards more s-state density. The Debye temperature of the impurity atoms is lower than for substitutional sites.

The impurity atoms are found in an electronically similar structure (line 3′) after a high-temperature annealing (~1200 K). This is attributed to a decoration of extended defect structures by Sb impurity atoms. The Debye temperature of the impurity atoms in this structure is found to be higher than for a substitutional site.

Line 4 is assigned to Sn atoms in interstitial agglomerates with silicon self-interstitials or further impurity atoms (at least after high-temperature annealings). The electronic configuration of the Sn atoms is close to the atomic $5s^25p^2$ configuration. The electron density at the nucleus is influenced by a compression of the impurity atoms. The Debye temperature is slightly higher than for substitutional sites.

Line 5 is assigned to Sn atoms replacing oxygen in a bent-bond configuration. In these defects the Sn atoms are approximately in an $5s^2$ configuration with bonds to two nearest Si neighbors. These structures are expected to contain vacancies and possibly oxygen. The Debye-Waller factor at room temperature is found to be lower than that of the vacancy-defect structure of line 3.

The defect structures of lines 3, 4, and 5 are found to anneal at ~700 K when associated with Sb-impurity atoms after the decay of ^{119m}Te. When associated with the Te atoms, for a heating up to ~1400 K, no annealing is observed. In the annealing and postimplantation experiments, the different behavior of the Sb and Te atoms in related defect structures could be studied by utilizing the decay chain $^{119m}\text{Te} \rightarrow {}^{119}\text{Sb} \rightarrow {}^{119}\text{Sn}$. The benefits of this method, demonstrated for the first time in this series of experiments, may be useful for microscopic investigations of impurity associated defect structures in other materials. In particular, it offers the possibility to study defect structures by means of the hyperfine interaction and the f factors of impurity atoms in daughter structures. Structures may be studied that are not necessarily formed in implantations of the daughter atoms as demonstrated here (and in Part I) for the decay chain $^{119m}\text{Te} \rightarrow {}^{119}\text{Sb} \rightarrow {}^{119}\text{Sn}$.

A strong interaction of O atoms with the vacancy defect structures of line 3 and the interstitial structure of line 4 is observed. These interactions are attributed to a large affinity of the O atoms to trap vacancies and interstitials, respectively, to form complicated defect structures.

In summary, the experiments reported in Part I and II of this paper show that the complex impurity-defect structures created by ion implantation can be studied by Mössbauer spectroscopy of the impurity atoms. The defect structures could be characterized by the hyperfine interaction and the f factor of the impurity atoms. In contrast to other hyperfine interaction measurements, all parameters of all implanted atoms are measured simultaneously. It should be noted that the method is applicable in all materials, however, the number of "Mössbauer isotopes" is limited.

ACKNOWLEDGMENTS

The authors would like to thank Dr. E. Antoncik and Dr. B. I. Deutch for helpful discussions and their interest in this work. We are grateful to the members of the cyclotron staff, N. O. Roy Poulsen and V. Voetmann, The Niels Bohr Institute, for having provided us with a large number of irradiations. This work has been supported by the Danish Natural Science Research Council.

---

*Present address: Central Bureau of Nuclear Measurements, Geel, Belgium.

[1]T. F. Lee, R. D. Pashley, T. C. Mc Gill, and J. W. Mayer, J. Appl. Phys. 46, 381 (1975).

[2]S. T. Picraux, N. G. E. Johansson, and J. W. Mayer, in *Semiconductor Silicon*, edited by R. R. Haberecht and E. L. Kern (Electrochemical Society, New York, 1969), p. 422.

[3]H. G. Grimmeiss, Ann. Rev. Mater. Sci. 7, 341 (1977).

[4]J. Guylai, O. Meyer, and J. W. Mayer, in *Ion Implantation*, edited by L. T. Chadderton and F. Eisen (Gordon and Breach, New York, 1971), p. 297.

[5]O. Meyer, N. G. E. Johansson, S. T. Picraux, and J. W. Mayer, Solid State Commun. 8, 529 (1970).

[6]D. W. Hafemeister and H. de Waard, Phys. Rev. B 7, 3014 (1973).

[7]G. Weyer, B. I. Deutch, A. Nylandsted Larsen, J. U. Andersen, and H. L. Nielsen, J. Phys. (Paris) 35, C6-297 (1974).

[8]H. de Waard, in *Proceedings of the International Conference on Hyperfine Interactions Studied in Nuclear Reactions and Decays, Uppsala, 1974*, edited by E. Karlsson and R. Wäppling (Almquist and Wiksell, Stockholm, 1975), p. 157.

[9]G. Vogl, J. Phys. (Paris) 35, C6-165 (1974).

[10]P. Boolchand, M. van Rossum, G. Langouche, J. Odeurs, H. Pattyn, and R. Coussement, Hyper. Inter. 2, 371 (1976).

[11]G. Weyer, A. Nylandsted Larsen, B. I. Deutch, E. Antoncik, and H. Loft Nielsen, in *Radiation Effects in Semiconductors*, edited by N. B. Urli and J. W. Corbett (Institute of Physics, Bristol, 1977), p. 491.

[12]A. Nylandsted Larsen, G. Weyer, B. I. Deutch, E. Antoncik, and H. Loft Nielsen, J. Phys. (Paris) 37, C6-883 (1976).

[13]G. Weyer, J. U. Andersen, B. I. Deutch, J. A. Golovchenko, and A. Nylandsted Larsen, Radiat. Eff. 24, 117 (1975).

[14]G. Weyer, A. Nylandsted Larsen, B. I. Deutch, J. U. Andersen, and E. Antoncik, Hyper. Inter. 1, 93 (1975).

[15]D. W. Palmer, in *Radiation Effects in Semiconductors*, edited by N. B. Miliard and J. W. Corbett (Institute of Physics, Bristol, 1977), p. 144.

[16]S. S. Cohen, R. H. Nussbaum, and D. G. Howard, Phys. Rev. B 12, 4095 (1975).

[17]See, for example, V. I. Goldanskii and E. F. Makarov, in *Chemical Applications of Mössbauer Spectroscopy*, edited by V. I. Goldanskii and R. H. Herber (Academic, New York, 1968), p. 34.

[18]Yu. Kagan and Ya. Iosilevskii, Sov. Phys. JETP 15, 182 (1962); 17, 195 (1963).

[19]G. Dearnaley, J. H. Freeman, R. S. Nelson, and J. Stephen, *Ion Implantation* (North-Holland, Amsterdam, 1973), p. 102.

[20]J. W. Mayer, L. Eriksson, and J. A. Davies, *Ion Implantation in Semiconductors* (Academic, New York, 1970), p. 71.

[21]H. de Waard, S. Bukshpan, and G. J. Kemerink, Hyper. Inter. 5, 45 (1977).

[22]M. van Rossum, J. de Bruyn, G. Langouche, R. Coussement, and P. Boolchand, J. Phys. (Paris) 37, C6-889 (1976).

[23]G. L. Latshaw, C. D. Sprouse, R. B. Russel, G. M. Kalvius, and S. S. Hanna, Bull. Am. Phys. Soc. 13, 1649 (1968).

[24]G. L. Latshaw, Ph.D. thesis (Stanford University, 1971) (unpublished).

[25]J. A. Sawicki, B. Sawicka, S. Lazarski, and E. Maydell-Ondrusz, Phys. Status Solidi B 57, K143 (1973).

[26]G. Weyer, B. I. Deutch, A. Nylandsted Larsen, and O. Holck, in *Proceedings of the International Conference on Mössbauer Spectroscopy, Cracow, 1975*, edited by A. Z. Hrynkiewicz and J. A. Sawicki (Akademia Gorniczo-Hutnicza, Cracow, 1975), p. 213.

[27]G. Weyer, G. Grebe, A. Kettschau, B. I. Deutch, A. Nylandsted Larsen, and O. Holck, J. Phys. (Paris) 37, C6-893 (1977).

[28]B. D. Sawicka and J. A. Sawicki, Phys. Lett. A 64, 311 (1977).

[29]G. Langouche, I. Dezsi, M. van Rossum, J. de Bruyn, and R. Coussement, Phys. Status Solidi B 89, K17 (1978).

[30]E. Antoncik, in *Proceedings of the International Conference on Lattice Defects in Semiconductors, Freiburg, 1974*, edited by F. A. Huntley (Institute of Physics, Bristol, 1975), p. 23.

[31]E. Antoncik, Hyper. Inter. 1, 329 (1976).

[32]L. T. Chadderton and F. H. Eisen, in *Ion Implantation*, edited by L. T. Chadderton and F. Eisen (Gordon and Breach, New York, 1971), p. 445.

[33]J. F. Gibbons, in *Ion Implantation*, edited by L. T. Chadderton and F. Eisen (Gordon and Breach, New York, 1971), p. 343.

[34]Young-Hoon Lee and J. W. Corbett, Phys. Rev. B 13, 2653 (1976).

[35]J. W. Corbett, R. S. McDonald, and G. D. Watkins, J. Phys. Chem. Solids 25, 873 (1964).

[36]K. Matsui, R. R. Hasiguti, T. Shoji, and O. Ahkawa, in *Proceedings of the International Conference on Lattice Defects in Semiconductors, Freiburg, 1974*, edited by F. A. Huntley (Institute of Physics, Bristol, 1975), p. 572.

[37]A. Brelot, IEEE Trans. Nucl. Sci. 19, 220 (1972).

[38]H. Stein, Radiat. Eff. 9, 195 (1971).

[39]G. D. Watkins, Phys. Rev. B 12, 4383 (1975).

[40]M. Cordey-Hayes, J. Inorg. Nucl. Chem. 26, 915 (1964).

[41]H. Micklitz and P. H. Barret, Phys. Rev. B 5, 1704 (1972).

[42]J. K. Lees and P. A. Flinn, J. Chem. Phys. 48, 882 (1968).

[43]K. Weiser, Phys. Rev. 126, 1427 (1962).

[44]A. Brelot, in *Proceedings of the International Conference on Defects in Semiconductors, Reading, 1972*, edited by J. E. Whitehouse (Institute of Physics, Bristol, 1973), p. 191.